Enhancement of X-Ray Images for Cargo and Pallet Search Using FPCNN

[1]Ahmed G. Mahgoub, [2]Ziad A. El-Sahn, [3]Hossam-El-Deen M. Abdel-Baky, and [4]El-Sayed A. El-Badawy

[1, 2, 3, 4] Department of Electrical Engineering, Faculty of Engineering, Alexandria University, Alexandria, 21544, Egypt.

[1, 2] Département de Génie Électrique et Informatique, Université Laval, Québec, QC, G1K 7P4, Canada.

[1] Research & Development Department, Palamar-Misr, Giza, Egypt.

[4] Alexandria Higher Institute of Technology, Alexandria, 21411, Egypt.

ABSTRACT

In this paper the feedback pulse coupled neural network (FPCNN) is used for the segmentation and edge detection of x-ray images generated from American Science and Engineering (AS&E) Inc. systems used for cargo and pallet search. We prove that this technique is able to isolate important parts of x-ray images. Furthermore, our results show that the FPCNN has a good ability to retrieve small density variations which is one of the main goals of x-ray inspection.

Keywords: Edge detection, Feedback Pulse Coupled Neural Network (FPCNN), PCNN, segmentation, X-ray.

1. INTRODUCTION

With the development of international trade and the change of international situation, customs departments all over the world are paying more attention to the security and facility of trade as well as inspecting contraband goods. To defend against terrorism and to safeguard the security of homelands, detecting weapons of mass destruction (WMD), dirty bombs and radioactive materials has become one of the compulsory functions of the container/vehicle inspection systems demanded by customs [1].

The use of the Feedback Pulse Coupled Neural Network (FPCNN) model for x-ray images enhancement is a result of a work that is started due to the advice of the operators in most sites who are using the x-ray to inspect the goods and cargos. For the large images where the scanned target is a container or many goods packed in one package, the image is very complicated to be studied, and hard to be tested, as the operator's eye swings all over the image and he cannot concentrate on a certain part, also the operator is confused due to the huge change in densities that make it hard to isolate a suspected target.

The visual cortex is the part of the brain that processes the information from the eye. The Pulse Coupled Neural Network (PCNN) is a synthetic model for image processing which mimics the visual cortex of mammals. The PCNN developed from studies of the visual cortex of small mammals made by e.g. Eckhorn *et al.* [2] is shown in Fig. 1. These studies have led to the creation of new algorithms that are achieving new levels of sophistication in electronic image processing.

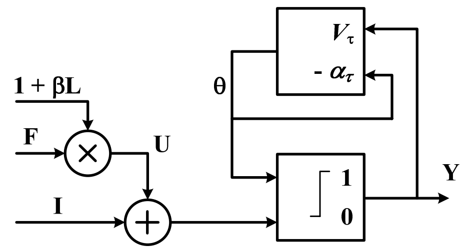

Fig. 1. The basic PCNN neuron.

2. PCNN MODEL AND CHARACTERISTICS

In the next equations we will refer to n as being the current iteration (discrete time step) where n varies from 1 to N-1 (N is the total number of iterations; n = 0 is the initial state). The dendritic tree can be described by the following equations [3]:

$$F_{ij}[n] = e^{-\alpha F}.F_{ij}[n-1] + V_F.\sum_{kl} M_{ijkl} Y_{kl}[n-1] + S_{ij} \tag{1}$$

$$L_{ij}[n] = e^{-\alpha L}.L_{ij}[n-1] + V_L.\sum_{kl} W_{ijkl} Y_{kl}[n-1] \tag{2}$$

$$U_{ij}[n] = F_{ij}[n]\{1+\beta L_{ij}[n]\} \tag{3}$$

$$Y_{ij}[n] = \begin{cases} 1, if\ U_{ij}[n] > \theta_{ij}[n-1] \\ 0, \text{otherwise} \end{cases} \tag{4}$$

$$\theta_{ij}[n] = e^{-\alpha_\theta}.\theta_{ij}[n-1] + V_\theta.Y_{ij}[n] \tag{5}$$

The original PCNN model is also called a three-oscillator model, this name is derived from the behavior of the neurons during the iteration process, the feeding, linking and the threshold equations give this oscillation behavior. A typical behaviour is shown in Fig. 2.

Feedback PCNN

It was found that the amount of feedback in a cat's brain is actually higher than the amount of feed forward processing. The feedback supplies information to resolve any conflicts that may exist and it enhances features by changing the pre processing parameters for intermediate inputs.

In the feedback PCNN, output information is sent back to the input. The outputs are collected as a weighted time average A, in a fashion similar to the computation of θ

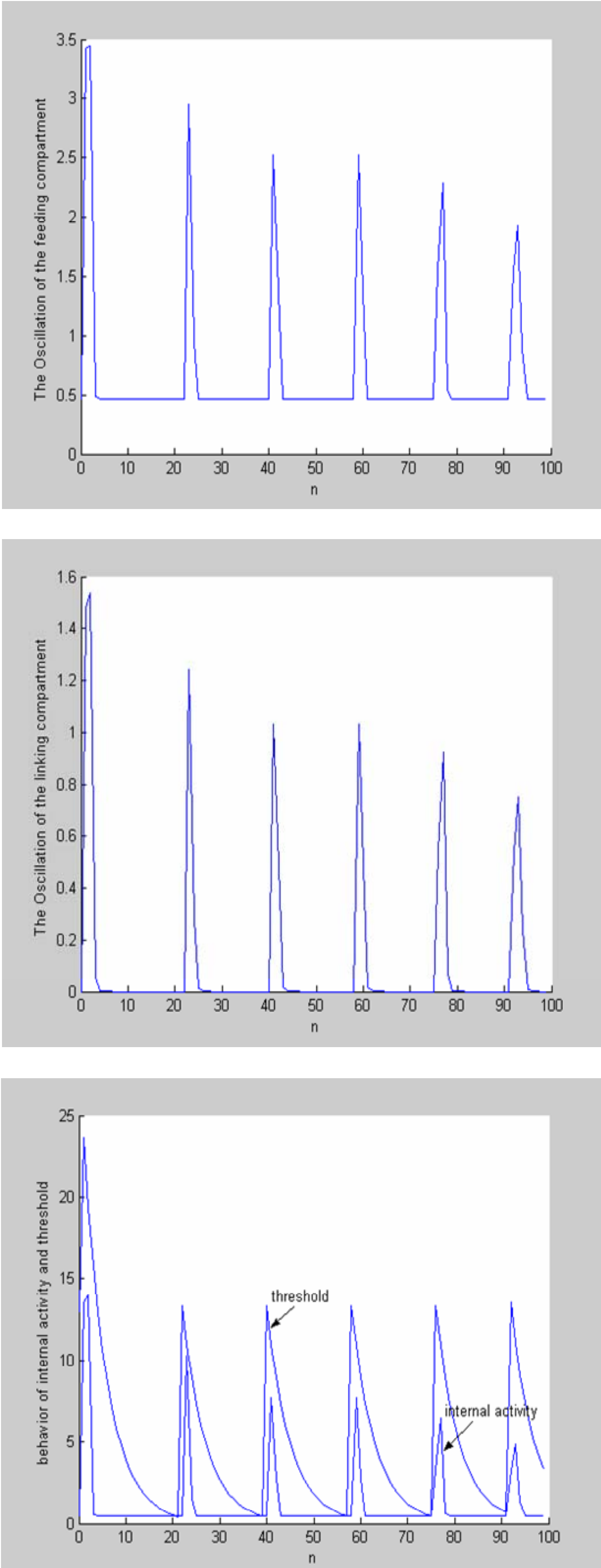

Fig. 2. The Oscillation of the F, L, and the behavior of the internal activity and the threshold of the neuron. Note: This neuron is the (200,200) neuron in a 480×480 x-ray image from AS&E library [4].

except for the constant *V*. The two introduced equations are:

$$A[n] = A[n-1].e^{-\alpha_A} + V_A.Y[n-1] \tag{6}$$

$$S_{ij}[n] = S_{ij}[n-1]/A_{ij}[n-1] \tag{7}$$

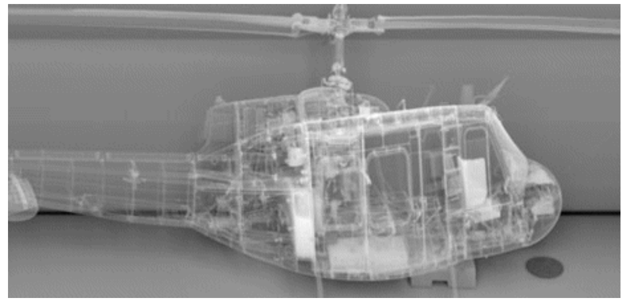

Fig. 3. Original image of helicopter.

where the two new parameters α_A, and V_A are introduced. The input of the PCNN is modified by the second equation for each iteration n and the result for the feedback PCNN case is obtained by iterating the normal five equations combined with the two new ones[5].

The feedback PCNN introduces one more oscillation equation that makes the algorithm consumes more time for the overall iterations, but it can give some important new outputs more than the other algorithms.

3. SEGMENTATION AND EDGE DETECTION

There is no theory of image segmentation. As a consequence, no single standard method of image segmentation has emerged. Rather, there are a collection of ad hoc methods that have received some degree of popularity.

One of the commonly used methods for segmentation is the thresholding transformation, that sets each gray level that is less than or equal to some prescribed value *T* called the threshold value-to zero, and each level greater than *T* is changed to *K*-1, where *K* is the greatest gray level value [6]. The thresholding transformation is defined by

$$g(x,y) = \begin{cases} 0 & \text{if } g(x,y) \le T \\ K-1 & \text{if } g(x,y) > T \end{cases} \tag{8}$$

Or, the output can be reversed.

An edge in a continuous domain edge segment can be detected by forming the continuous one-dimensional gradient along a line normal to the edge slope, which is at an angle with respect to the horizontal axis. If the gradient is sufficiently large (i.e., above some threshold value), an edge is deemed present [7].

The gradient of the continuous image *g*(*x*,*y*) is defined to be the ordered pair of partial derivatives as follows

$$\nabla g(x,y) = (\frac{\partial g}{\partial x} g(x,y), \frac{\partial}{\partial y} g(x,y)) \tag{9}$$

As the gradient indicates the rate of change in gray level in the image in the x and y directions, the magnitude M of ht gradient is defined by

$$M = \sqrt{(\frac{\partial}{\partial x} g(x,y))^2 + (\frac{\partial}{\partial y} g(x,y))^2} \tag{10}$$

Figures 4 and 5 are the segmented and edge detected versions, respectively of the helicopter shown in Fig. 3 which is scanned using AS&E systems. In order to obtain clear edges as illustrated in Fig. 5, the image should first be segmented.

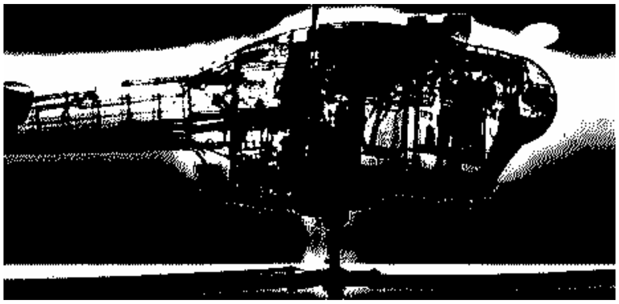

Fig. 4. Threshold segmentation method.

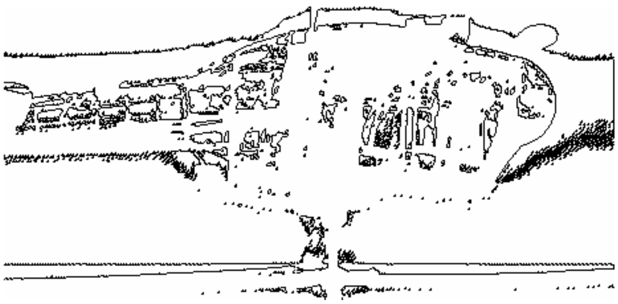

Fig. 5. Gradient edge detection method.

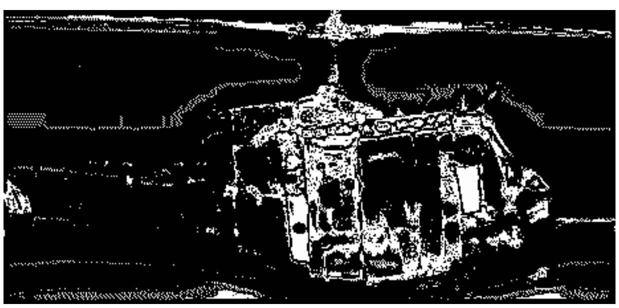

Fig. 6. Segmentation of helicopter body.

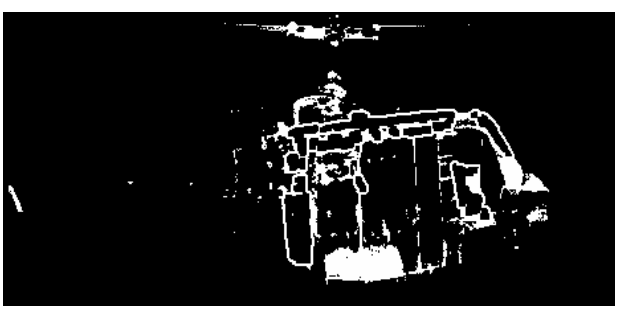

Fig. 7. Edges of helicopter using FPCNN.

Figures 6 and 7 show the FPCNN segmentation and edge detection of Fig. 3. It can be shown that the FPCNN gives better segmentation and edge detection for the body of the helicopter compared to the threshold technique shown in Figs. 4 and 5. It is important to note that the result in Fig. 7 corresponds to an output image of only one iteration of the FPCNN; therefore the details of the helicopter 'tail' and/or other parts can be viewed in other images from other iterations. This property can be illustrated in Fig. 8, where the fuel tank of the helicopter

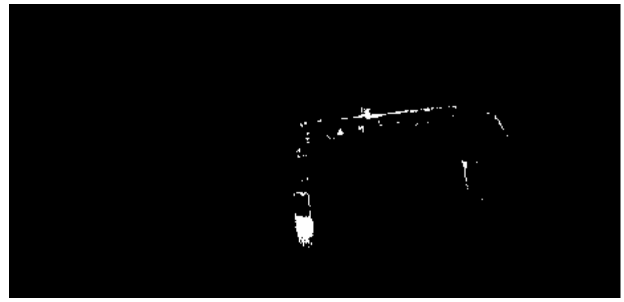

Fig. 8. The fuel tank is isolated using FPCNN.

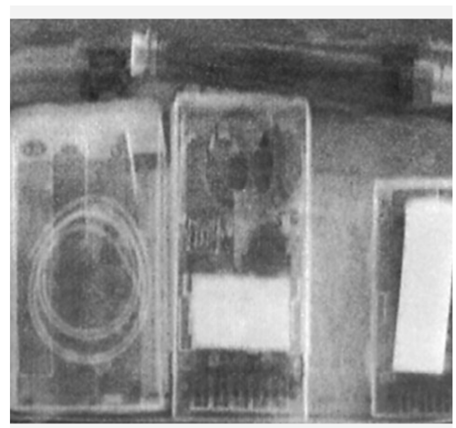

Fig. 9. A scanned suitcase.

Fig. 10. The segmented image of Fig. 9 using FPCNN.

is separated from its surrounding parts. This can be very useful for post-inspection.

Another example showing the ability of the FPCNN to segment the x-ray images is the backscatter image of a suitcase (Fig. 9) containing 8.5 feet of live detonation cord, 4 ounces of plastic explosives and a half-pound of live C4 plastic explosives that have been hidden among the cluttered contents [4]. Figure 10 shows the ability of the FPCNN to segment the two explosives and the cord.

4. DETECTING SMALL DENSITY VARIATIONS

Some of the FPCNN outputs have the ability to segment the suspected objects that the man-eye cannot distinguish

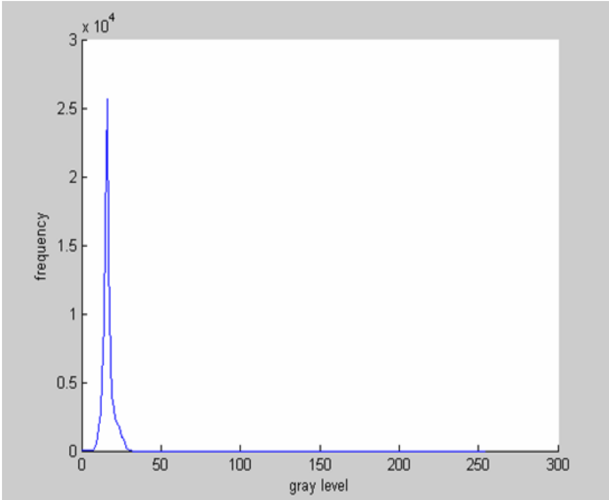

Fig. 11. Histogram of the original image of Fig. 3.

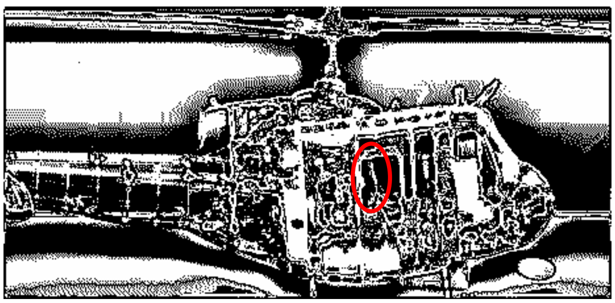

Fig. 12. A FPCNN output.

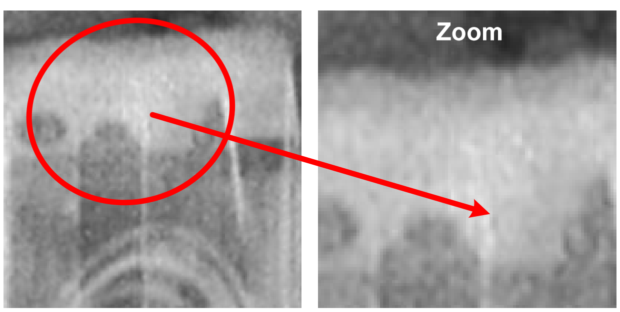

Fig. 13. The metal part that has the change density.

from the surroundings. From the original image of the helicopter, it can be seen that the gray level is nearly the same for all pixels; this may be due to the use of a Log scale filter before displaying the image. The histogram of the helicopter in Fig. 3 is shown in Fig. 11.

Note that in Fig. 11, the '0' gray level corresponds to the brightest pixel (i.e. white color). Because of the low contrast in the original image, it is hard for the operators to inspect backscatter images.

Figure 12 shows the output of another FPCNN iteration where more details about the structure of the 'tail' of the helicopter are shown and where its body is segmented differently. Moreover, the circled area in the image represents the segmentation of a part (vertical part near the door of the helicopter) which has nearly the same gray level as the background.

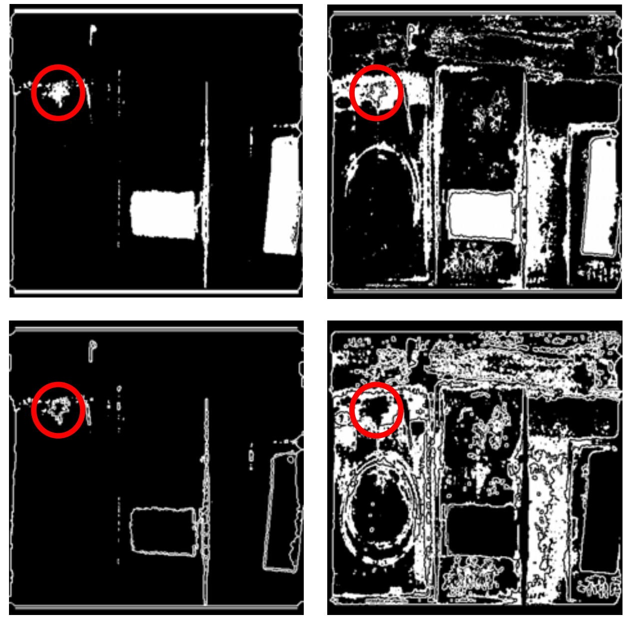

Fig. 14. Four FPCNN outputs showing the slight density variations for the metal part.

The image of the suitcase that contains the explosives and the cord (Fig. 9), has an interesting variation in density that is very hard to detect using the man-eye, this change is not between two different materials, but inside the same material. Figure 13 shows the examined part and a zoomed version of it. The corresponding FPCNN output images are illustrated in Fig. 14 where the circles show the location of that variation.

5. CONCLUSIONS AND FUTURE WORK

In this paper FPCNN was used to enhance x-ray images of cargos and pallets generated from AS&E systems. This technique has shown good results in both segmentation and edge detection. As a result, the aforementioned technique suits well for x-ray operators where they can inspect scanned images in a clear segmented version as well as an improved inspection for the edges. We have also shown that the most promising result is the ability to detect slight density variations that cannot be detected using man-eye.

According to the FPCNN algorithm presented in [5], the iteration output is only 2-level (2-class segmentation). When compared to other techniques having the same number of classes (i.e. 2-class), it proves to be more effective due to the large number of output segmented images (corresponding to different iterations) that contain different segmented areas and edges, which helps the operators doing their job in a better way.

As a result of the implementation of the FPCNN and the huge number of iterations, it takes a considerable time to output the images. This may not be critical during the inspection of a suspected image. On the other hand, for real-time applications the time factor is vital; so future work may be aimed to implement the FPCNN algorithm on field programmable gate arrays (FPGAs) to benefit from parallel processing. Other technologies such as application specific integrated circuits (ASICs) may be considered to make the iteration process faster.

6. ACKNOWLEDGMENT

The authors thank Mr. Shereen Ezat the general manager of Palamar-Misr for his effort and support to complete this work.

7. REFERENCES

[1] Dr. Jianmin LI, Lin YANG & Xiaoyi HE, “Advanced X-ray container/vehicle inspection systems plus radiation detection subsystem: THSCAN™ fused technology,” **Nuctech**, Beijing, China, 2006.

[2] R. Eckhorn, H.J. Reitboeck, M. Arndt, and P. Dicke, “Feature Linking via Synchronization Among Distributed Assemblies,” **Neural Computing 2**, 1990, pp. 293-307.

[3] Taymoor M. Nazmy “Comparing the Time Signals of the PCNN Models for Implementation in Face Recognition,” The 9th World Multi-conference on Systemics, Cybernetics, and Informatics **(WMSCI 2005)**, Orlando, USA, 2005.

[4] www.as-e.com

[5] V. Beèanovic, “Signal and Image Processing in Engineering Physics,” Ph.D. Thesis, **Royal Institute of Technology** (KTH), Stockholm, 2000.

[6] Earl Gose, and Richard Johnsonbaugh, *Pattern Recognition and Image Analysis*, Prentice Hall PTR, Upper Saddle River, NJ, 07458, 1996.

[7] William K. Pratt, *Digital Image Processing*, 3rd Edition, John Wiley & Sons, Inc., 2001.